$$S^0_{\frac{1}{3}\frac{1}{3}0} = -\frac{1}{a^3}\left(\frac{8\pi}{\sqrt{3}} + \frac{2}{\sqrt{\pi}}\sum_{\lambda_1\lambda_2}\Gamma(\tfrac{3}{2}, \pi\sigma^2_{\lambda,j})\sigma^{-3}_{\lambda,j} + \frac{4\pi\sqrt{\pi}}{\sqrt{3}}\sum_i n_i h_i c_i \Gamma(-\tfrac{1}{2}, \pi h_i^2)\right) . \quad \text{(A8)}$$

The $\Gamma(n, x)$ are the incomplete Γ functions, the sum over $\lambda_1\lambda_2$ is on a direct-space planar hexagonal lattice, and $\sigma_{\lambda,j}$ are magnitudes of vectors from the origin to the points of that lattice. Note that in Eq. (A7) the $\lambda_1 = \lambda_2 = 0$ term is excluded from the sum whereas it is included in Eq. (A8). Both Eq. (A7) and Eq. (A8) are independent of the axial ratio α and are therefore simply numbers whose value need be calculated only once. Since Eq. (A7) also occurs for hcp lattices, de Wette[6] has calculated this number. We have chosen to recalculate it as a check. Terms in the direct lattice sum were included up to $|\sigma_{\lambda j}| = 10$, and the number of terms in the sum were reduced by taking advantage of the threefold symmetry in the hexagonal lattice. The value obtained was $a^3 S^0_{000} = -11.034176$, which is to be compared with de Wette's value[6] of -11.0341754. Similarly, the value obtained for Eq. (A8) was $a^3 S^0_{\frac{1}{3}\frac{1}{3}0} = -23.150541$. The remaining sums, $S^{\lambda 3}_{\frac{1}{3}\frac{1}{3}0}$, $S^{\lambda 3}_{000}$, and $S_{\frac{1}{3}\frac{1}{3}\frac{1}{2}}$ were computed for a range of values in α and inserted in Eqs. (A2a) and (A2b) to yield the curves described in the text. Table III lists some of the results of the calculations. In all cases where possible, comparison of these results with those of Ref. 6 was excellent.

[1] E. N. Kaufmann, second preceding paper, Phys. Rev. B **8**, 1382 (1973).
[2] E. N. Kaufmann, first preceding paper, Phys. Rev. B **8**, 1387 (1973).
[3] J. C. Jamieson, Science **140**, 72 (1963).
[4] S. Andersson, Ark. Kemi **15**, 247 (1960).
[5] R. W. Sommerfeldt, T. W. Cannon, L. W. Coleman, and L. Schecter, Phys. Rev. **138**, B763 (1965); P. H. Stelson and F. K. McGowan, Phys. Rev. **105**, 1346 (1957).
[6] F. W. de Wette, Phys. Rev. **123**, 103 (1961).
[7] F. W. de Wette and G. E. Schacher, Phys. Rev. **137**, A78 (1965); Phys. Rev. **137**, A92 (1965).
[8] R. M. Sternheimer, Phys. Rev. **80**, 102 (1950); Phys. Rev. **84**, 244 (1952); Phys. Rev. **86**, 316 (1954); Phys. Rev. **95**, 736 (1954); Phys. Rev. **105**, 158 (1957); Phys. Rev. **130**, 1423 (1963).
[9] J. E. Doherty and D. F. Gibbons, Acta Metall. **19**, 275 (1971).
[10] L. Pauling, in *Theory of Alloy Phases* (American Society for Metals, Cleveland, 1956).
[11] F. D. Feiock and W. R. Johnson, Phys. Rev. **187**, 39 (1969).
[12] J. Pelzl, Z. Phys. **251**, 13 (1972).

PHYSICAL REVIEW B VOLUME 8, NUMBER 4 15 AUGUST 1973

Analysis of the Lattice Specific Heat of Mo:Re Alloy

M. D. Tiwari and Bal K. Agrawal
Department of Physics, University of Allahabad, Allahabad 211002, India

The low-temperature lattice specific heat of a Mo- 5-at.%-Re alloy has been successfully explained on the basis of a Green's-function theory. We take into account the effects due to change in mass at the substitutional impurity site and also the changes in the nearest-neighbor central and noncentral force constants for the impurity–host-crystal interaction. The enhanced specific heat is dominated by force-constant changes and very much sensitive to these changes. It is observed that the contribution of the even parity A_{1g}, E_g, F_{1g}, and F_{2g} modes are very significant and, in fact, dominate over that of F_{1u} symmetry modes in the low-temperature side of the specific-heat curve. However, at higher temperatures more resonance modes appearing in F_{1u} irreducible representation are excited and their contribution dominates over all others. The present values of the defect parameters are found to be quite similar to those obtained earlier by elastic-constant data.

I. INTRODUCTION

The effects of impurities on the vibrational properties of solids has been studied by performing different types of experiments,[1] e.g., measurement of lattice specific heat,[2–4] elastic constants,[5] infrared absorption,[6] inelastic neutron scattering,[7] etc. Usually a localized perturbation model for the defect is assumed to explain these experiments. It is therefore of much interest to determine the defect parameters for a particular host-impurity system which should be able to explain two or more of such experiments. In an earlier work, the elastic constants of Mo: Re alloys measured by Davidson and Brotzen[8] were analyzed by Kesharwani and Agrawal[9] to determine the parameters of a nearest-neighbor-defect model for a rhenium impurity atom in a molybdenum matrix. In the present paper we discuss the lattice-specific-heat measurements made by Morin and Maita[10] on the same system, i.e., Mo: Re (5-at % Re) alloy.

In the specific-heat measurements it is difficult

to detect the occurrence of localized modes because they are not excited at low temperatures. But the low-frequency resonance mode gives rise to an appreciable contribution to the specific heat at low enough temperatures. In an earlier communication[11] the present authors have theoretically studied the appearance of the resonance mode due to heavy silver impurity atoms in aluminum crystals and have shown the importance of force-constant changes in understanding the experimental data.

A brief account of the theory of the lattice specific heat in an imperfect crystal is given in Sec. II A. The localized perturbation model is described in Sec. II B. The Green's functions and the enhanced specific heat are computed in Secs. III A and III B, respectively. The results are summarized in Sec. IV.

II. THEORY

A. Lattice Specific Heat

The lattice specific heat of a solid at temperature T containing N atoms per gram mole is given by[11]

$$C_L(T)=\frac{\hbar^2}{4k_BT^2}\int_0^\infty \omega^2 N(\omega)\operatorname{csch}^2\frac{\hbar\omega}{2k_BT}\,d\omega\,, \qquad (1)$$

where $\hbar$ is Planck's constant, k_B is Boltzmann's constant, ω is the phonon frequency, and $N(\omega)d\omega$ is the number of phonon states lying in the interval ω to $\omega+d\omega$ in the limit $d\omega\to 0$.

The phonon density of states is changed by the introduction of defects. For a symmetric perturbation this change in density of states can be expressed as the sum of contributions from the various irreducible representations occurring in the problem in hand. We may, therefore, write for the change at specific heat

$$\Delta C_L(T)=\sum_\nu \Delta C_L^\nu(T)\,, \qquad (2)$$

where $\Delta C_L^\nu(T)$ is the contribution from the irreducible representation ν.

The problem is much simplified if we introduce phase shifts δ_ν which are defined by

$$\tan\delta_\nu=-\frac{\mathrm{Im}D_\nu(z)}{\mathrm{Re}D_\nu(z)}\,, \qquad (3)$$

where $D_\nu(z)=|\underline{I}+\underline{g}_\nu(z)\underline{P}_\nu(\omega^2)|$ is the resonance denominator in the irreducible representation ν. $\underline{I}$ is the unit matrix, $\underline{P}_\nu(\omega^2)$ and $\underline{g}_\nu(z)$ are the perturbation and Green's-function matrices projected onto the subspace of the irreducible representation ν, and z is the complex squared frequency given as $z=\omega^2+2i\omega\xi$ in the limit $\xi\to 0$. For a crystal containing a low concentration of randomly distributed impurities one may determine the change in specific heat due to a single defect and multiply it by the number of defects present in the solid.

After integrating Eq. (1) once by parts and introducing the phase shifts we obtain

$$\Delta C_L(T)=-\sum_\nu \frac{2k_BcNB^2}{\pi}\int_0^\infty \delta_\nu\omega\,\operatorname{csch}^2B\omega \times(2-B\omega\coth B\omega)\,d\omega\,, \qquad (4)$$

where $B=\hbar/2k_BT$ and c is the fractional impurity concentration.

B. Perturbation Model

The crystal structures of molybdenum and its alloys with rhenium atoms are body-centered cubic containing one atom per unit cell. The point-group symmetry of a substitutional impurity is O_h. We assume a nearest-neighbor perturbation model in which we take into account the changes in the central and noncentral interactions along with the mass change at the impurity site. The matrix $\underline{P}(\omega^2)$ is of dimension 27×27. The resonance denominator has been analyzed in an earlier paper[12] for a more general lattice, i.e., CsCl structure. The irreducible representations in the present problem are F_{1u}, F_{2u}, F_{1g}, F_{2g}, E_g, E_u, A_{1g}, and A_{2u}. For a monatomic bcc lattice the resonance denominators for the various irreducible representations are given by

$$D_{F_{1u}}(z)=D_1(D_5D_9-D_6D_8)-D_2(D_4D_9-D_6D_7)+D_3(D_4D_8-D_5D_7)\,, \qquad (5)$$

with

$$D_1=1-\epsilon\omega^2g_1+8A'(g_1-g_2)-16B'g_3\,,$$
$$D_2=(\sqrt{8})\,[-\epsilon\omega^2g_2+A'(8g_2-x_1)-(\sqrt{2})x_3B']\,,$$
$$D_3=4\,[-\epsilon\omega^2g_2+A'(8g_3-x_3/\sqrt{2})-B'x_2]\,,$$
$$D_4=-(\sqrt{8})\,[A'(g_1-g_2)-2B'g_3]\,,$$
$$D_5=1+A'(x_1-8g_2)+(\sqrt{2})B'x_3\,,$$
$$D_6=A'[x_3-8(\sqrt{2})g_3]+2B'x_2\,,$$
$$D_7=4[B'(g_2-g_1)+C'g_3]\,,$$
$$D_8=(\sqrt{2})B'(x_1-8g_2)+C'x_3\,,$$
$$D_9=1+(\sqrt{2})B'\,[x_3-8(\sqrt{2})g_3]+C'x_2\,,$$

where

$$x_1=g_1+2g_4+g_5+g_7+g_9+g_{10}\,,$$
$$x_2=g_1-g_5+g_6+g_7+g_8-g_9\,,$$
$$x_3=-(\sqrt{2})\,(g_6-g_8)\,,$$
$$A'=\tfrac{1}{3}(\lambda+2\lambda')\,,\quad B'=\tfrac{1}{3}(\lambda-\lambda')\,,\quad C'=\tfrac{1}{3}(2\lambda+\lambda')\,;$$
$$D_{F_{2u}}(z)=1+\lambda'(g_1-g_5-g_6+g_7-g_8-g_9)\,, \qquad (6)$$
$$D_{F_{1g}}(z)=1+\lambda'(g_1-g_5-g_6-g_7+g_8+g_9)\,, \qquad (7)$$

$$D_{F_{2g}}(z) = 1 + [g^{11}_{F_{2g}} \tfrac{1}{3}(\lambda + 2\lambda') + \tfrac{2}{3}(\sqrt{2})(\lambda - \lambda') g^{12}_{F_{2g}} + g^{22}_{F_{2g}} \tfrac{1}{3}(2\lambda + \lambda')] + \lambda\lambda' [g^{11}_{F_{2g}} g^{22}_{F_{2g}} - (g^{12}_{F_{2g}})^2] , \quad (8)$$

with

$$g^{11}_{F_{2g}} = g_1 + 2g_4 + g_5 - g_7 - g_9 - 2g_{10} ,$$

$$g^{22}_{F_{2g}} = g_1 - g_5 + g_6 - g_7 - g_8 + g_9 ,$$

$$g^{12}_{F_{2g}} = -(\sqrt{2})(g_6 + g_8) ;$$

$$D_{E_g}(z) = 1 + \lambda'(g_1 - 2g_4 + g_5 - g_6 - g_7 + g_8 - g_9 + 2g_{10}) , \quad (9)$$

$$D_{E_u}(z) = 1 + \lambda'(g_1 - 2g_4 + g_5 - g_6 + g_7 - g_8 + g_9 - 2g_{10}) , \quad (10)$$

$$D_{A_{1g}}(z) = 1 + \lambda(g_1 - 2g_4 + g_5 + 2g_6 - g_7 - 2g_8 - g_9 + 2g_{10}) , \quad (11)$$

and

$$D_{A_{2u}}(z) = 1 + \lambda(g_1 - 2g_4 + g_5 + 2g_6 + g_7 + 2g_8 + g_9 - 2g_{10}) . \quad (12)$$

Here λ (λ') is the change in mass-reduced nearest-neighbor central (noncentral) force constant and $\epsilon = (M' - M)/M'$ is the change in mass at impurity site, where M and M' denote the masses of the host and impurity atoms, respectively.

The various Green's functions are given by

$$g_\mu(z) = \frac{1}{N} \sum_{s=1}^{3} \sum_{\vec{k}} \frac{J_\mu(\vec{k}/s)}{\omega^2_{\vec{k},s} - z} , \quad (13)$$

where μ has values from 1 to 10, and $\omega_{\vec{k},s}$ is the phonon frequency corresponding to the wave vector $\vec{k}$ in the polarization branch s. The explicit expressions for $J_\mu(\vec{k}/s)$ required for the ten Green's functions have been given in Ref. 9.

III. NUMERICAL COMPUTATIONS AND RESULTS

A. Green's Functions

The lattice dynamics of molybdenum in Krebs's model[13] has been discussed by Kesharwani and Agrawal.[9] The eigenfrequencies and eigenvectors were determined for a uniformly distributed 8000 points in the first Brillouin zone. The calculated dispersion curves in the main symmetry directions were seen to be in good agreement with the experimental results of Woods and Chen.[14] The Green's functions were calculated by a staggered bin averaging procedure as described in Ref. 11. The pertinent integrations were performed after dividing the phonon frequency range into 60 equal bins, each of width 0.25 in the units of bin width.

B. Enhanced Specific Heat

At low temperatures (below 20 °K) the specific heats of molybdenum and its alloy with rhenium (5 at.%) have been measured by Morin and Maita.[10]

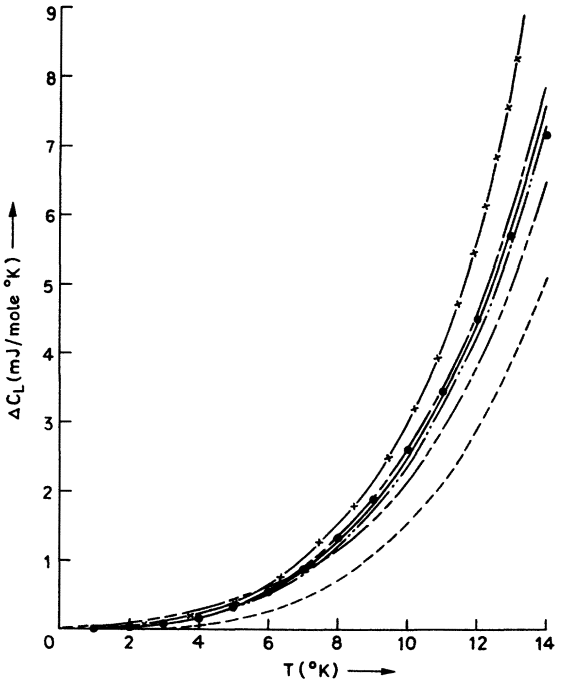

FIG. 1. Enhanced lattice specific heat in Mo–5-at.%-Re alloy. Experimental points (measured in 10^{26} sec^{-2}): ---, $\lambda = 0$, $\lambda' = 0$; ——, $\lambda = -1.0$, $\lambda' = 0$; —··—, $\lambda = 1.7$, $\lambda' = -0.8$; —, $\lambda = 1.65$, $\lambda' = -0.8$, ——, $\lambda = 1.60$, $\lambda' = -0.8$; —×—, $\lambda = 1.65$, $\lambda' = -1.0$.

The reliability of their result is better than ± 5%.[15] They have observed that the total specific heat of these systems may well be described by a T-dependent electronic contribution and a T^3-dependent lattice contribution. An enhancement of about 16% in lattice specific heat due to a concentration of 5-at.% Re of impurity atoms in molybdenum has been observed throughout the studied temperature range.

The change in lattice specific heat has been calculated by using Eq. (4), and the results are compared with the experimental data in Fig. 1. The contribution of mass defects to the change in measured specific heat is ~45% (see Fig. 1) and the rest of the specific-heat change arises because of the force-constant changes. Initially an attempt was made to fit the experimental curve with a central force-constant change λ but was found to be unsuccessful. The reason is that the mass change plus the central force-constant change give rise to essentially a T^2-dependent specific heat. As an example, we show the enhanced specific heat with $\epsilon = 0.9406$ and $\lambda = -1.0 \times 10^{26}$ sec^{-2} in Fig. 1.

The experimental curve was fitted by varying both the central and the noncentral force-constant changes λ and λ'. Some of the calculated curves for different sets of the parameters (λ, λ') have been depicted in Fig. 1. The impurity-induced

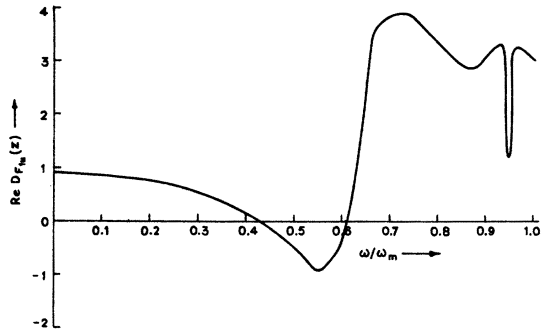

FIG. 2. Real part of the determinant appearing in the F_{1u} irreducible representation for the parameters $\lambda = 1.65 \times 10^{26}$ sec^{-2} and $\lambda' = -0.8 \times 10^{26}$ sec^{-2}. ω_m is the maximum frequency.

specific heat is quite sensitive to force-constant changes. For example, a 10% variation in λ induces an average change of ~5% in the whole temperature range of the enhanced specific heat, whereas a 10% variation in λ' gives rise to a corresponding change of ~15%. In general, the specific heat is approximately three times more sensitive to λ' than to λ in the full temperature range.

The best fit has been obtained with a unique set of parameters $\lambda = 1.65 \times 10^{26}$ sec^{-2} and $\lambda' = -0.8 \times 10^{26}$ sec^{-2}. They produce resonances at $\omega_{r1} = 123$ cm^{-1} and $\omega_{r_2} = 176$ cm^{-1}. The real part of the resonance denominator and the phase shifts in the F_{1u} irreducible representations have been plotted in Figs. 2 and 3. The main contributions to the specific heat come from F_{1u}, F_{1g}, F_{2g}, E_g, and A_{1g} irreducible representations. This behavior is quite different from that observed earlier[11] in the system Al: Ag, in which the changed specific heat is mainly determined by F_{1u} irreducible representations. At very low temperatures (~2 °K) the contributions of the F_{1g}, F_{2g}, E_g, and A_{1g} symmetry motions dominate over that of F_{1u} symmetry motions. The contribution of F_{1u} symmetry modes increases with an increase in temperature because of the excitation of the resonance modes and, in fact, dominates over all the other symmetry modes at comparatively higher temperatures. The contributions of these irreducible representations are depicted in Figs. 4 and 5.

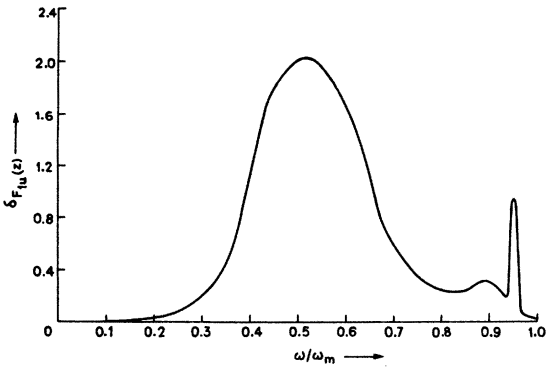

FIG. 3. Phase shifts in F_{1u} irreducible representation for $\lambda = 1.65 \times 10^{26}$ sec^{-2} and $\lambda' = -0.8 \times 10^{26}$ sec^{-2}. ω_m is the maximum frequency.

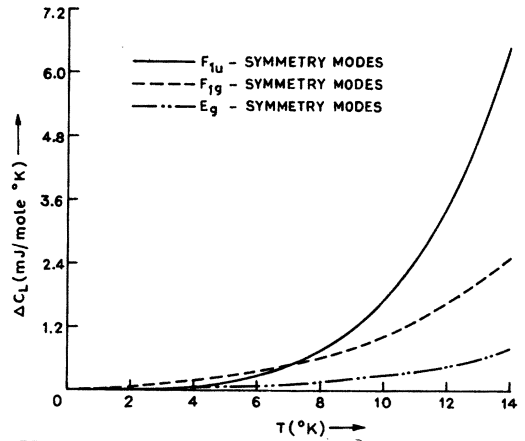

FIG. 4. Contribution to enhanced lattice specific heat due to F_{1u}, F_{1g}, and E_g symmetry modes for $\lambda = 1.65 \times 10^{26}$ sec^{-2} and $\lambda' = -0.8 \times 10^{26}$ sec^{-2}.

The present values of λ and λ' are very near to $\lambda = 1.648 \times 10^{26}$ sec^{-2} and $\lambda' = -0.661 \times 10^{26}$ sec^{-2} obtained earlier by Kesharwani and Agrawal using elastic-constant data. The values of the nearest-neighbor central and noncentral force constants and the next-nearest-neighbor central force constant for pure molybdenum are 3.77, −0.261, and 3.53×10^{26} sec^{-2}, respectively.

It may therefore appear that appreciable changes in the next-nearest-neighbor force constants could occur because of rhenium impurity atoms. However, a recent analysis[16] of the elastic-constant data of this host-impurity system based on a next-

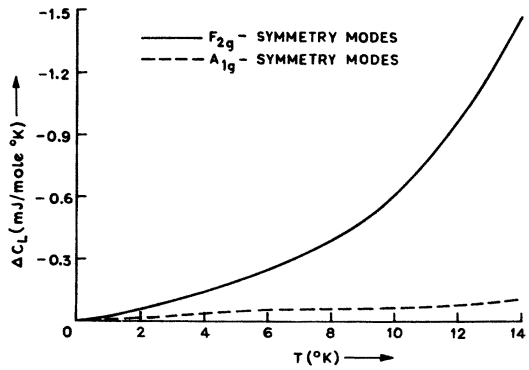

FIG. 5. Contribution to enhanced lattice specific heat due to F_{2g} and A_{1g} symmetry modes for $\lambda = 1.65 \times 10^{26}$ sec^{-2} and $\lambda' = -0.8 \times 10^{26}$ sec^{-2}.

nearest-neighbor (nnn) perturbation model has revealed that there occur only insignificant changes in the nnn force constants. Thus, the inclusion of two more unknown parameters (nnn force-constant changes) in the present theory which would further complicate the situation does not seem to be worthwhile.

IV. CONCLUSIONS

The lattice specific heat of Mo with 5-at.%-Re alloy in the temperature range 1–14 °K can be well understood on the basis of a nearest-neighbor perturbation model, after considering changes in the central and noncentral force constants for the impurity–host-crystal interaction. Above 14 °K, the calculated specific heat does not show a T^3-dependent behavior. The contribution of force-constant changes to the specific heat is seen to be quite large, i.e., ~55% of the total enhanced specific heat. The specific heat is very sensitive to force-constant changes, especially to the noncentral part. The contribution of all the even-parity modes, i.e., A_{1g}, E_g, F_{1g}, and F_{2g}, are quite large and dominate over the contribution of the odd-parity F_{1u} modes in the low temperature of the specific-heat curve. However, at higher temperatures more resonance modes are excited and the contribution of F_{1u} symmetry modes dominates.

ACKNOWLEDGMENTS

The authors are grateful to Professor Vachaspati for his interest in the present work. They are also thankful to the Computer Centre, I.I.T., Kanpur, for providing facilities on IBM 7044/1401 computers. M.D.T. expresses his thanks to K. M. Kesharwani for helpful discussions. B. K. A. is thankful to the University Grants Commission for financial assistance.

*Senior Research Fellow, Council of Scientific and Industrial Research, New Delhi.

[1]A. A. Maradudin, Solid State Phys. **18**, 273 (1966); Solid State Phys. **19**, 1 (1966).

[2]W. M. Hartmann, H. V. Culbert, and R. P. Huebener, Phys. Rev. B **1**, 1486 (1970).

[3]A. V. Karlsson, Phys. Rev. B **2**, 3332 (1970).

[4]B. A. Green, Jr. and A. A. Valladares, Phys. Rev. **142**, 379 (1966); T. B. Massalski and L. L. Isaacs, Phys. Rev. **138**, A139 (1965).

[5]B. J. Marshall and S. G. Ohara, Phys. Rev. B **3**, 4002 (1971).

[6]M. V. Klein, *Physics of Color Centres* (Academic, New York, 1968), Chap. 7.

[7]R. J. Elliot and A. A. Maradudin, *Neutron Inelastic Scattering* (International Atomic Energy Agency, Vienna, 1965), Vol. 1, p. 231; K. Lakatos and J. A. Krumhansl, Phys. Rev. **175**, 841 (1968); Phys. Rev. **180**, 729 (1969); K. M. Kesharwani and Bal K. Agrawal, Phys. Rev. B **6**, 2178 (1972); Phys. Rev. B **7**, 2378 (1973).

[8]D. L. Davidson and F. R. Brotzen, J. Appl. Phys. **39**, 5768 (1968).

[9]K. M. Kesharwani and Bal K. Agrawal, Phys. Rev. B **5**, 2130 (1972).

[10]F. J. Morin and J. P. Maita, Phys. Rev. **129**, 1115 (1963).

[11]M. D. Tiwari, K. M. Kesharwani, and Bal K. Agrawal, Phys. Rev. B **7**, 2378 (1973).

[12]Bal Krishna Agrawal, Phys. Rev. **186**, 712 (1969).

[13]K. Krebs, Phys. Rev. **138**, A143 (1965).

[14]A. D. B. Woods and S. H. Chen, Solid State Commun. **2**, 233 (1964).

[15]F. J. Morin (private communication).

[16]K. M. Kesharwani and Bal K. Agrawal, Phys. Rev. B (to be published.

PHYSICAL REVIEW B VOLUME 8, NUMBER 4 15 AUGUST 1973

Photoelectron Emission and the *d* Bands of Zinc and Cadmium

R. T. Poole, R. C. G. Leckey, J. G. Jenkin, and J. Liesegang
Physics Department, La Trobe University, Bundoora, Victoria, Australia 3083
(Received 21 August 1972; revised manuscript received 6 November 1972)

The *d* bands of Zn and Cd have been unambiguously located by photoelectron spectroscopy using 40.81-eV radiation. In Zn a single peak due to the $3d_{3/2,5/2}$ band of half-width 1.1 eV is found 9.5 eV below Fermi level, while for Cd, the $4d_{3/2,5/2}$ doublet is resolved at 10.2 and 11.1 eV below the Fermi level. The relevance of these results for band-structure calculations and for the interpretation of related optical and characteristic energy-loss experiments is discussed.

INTRODUCTION

The suitability of the helium-II resonance line at 40.81 eV as a probe for band-structure studies has recently been recognized.[1] Evidence available to date[2,3] suggests that the energy distributions of photoelectron spectra generated by Al $K\alpha$ radiation and by 40.81-eV helium resonance radiation are closely similar, and it is reasonable to assume that the spectra so generated are representative of the density of occupied states of the irradiated materials.[4] Without use of predispersion, the resolu-